# PACS photometer - Prime and Parallel scan mode release note

version 1.2

**The PACS ICC**

This document provides a summary of the inflight performance of the PACS scan map Astronomical Observing Template (AOT), its current status and calibration accuracy. The performance is judged to be suitable for scheduling observations made with 20″/sec (medium) and 60″/sec (fast) scan speeds in both the prime (nominal) and parallel mode with PACS in the high-gain and nominal bias configuration.

## Contents

# 1 Point spread function

The photometer PSF (see Figure 1) is characterised by:

- A narrow core which is round in the blue bands but slightly elongated in spacecraft Z direction in red.
- A tri-lobe pattern seen at the several % level in all bands, most clearly in the blue with its strongest signal, and ascribed to imperfect mirror shape.
- Knotty structure at sub-percent level, clearly seen in blue and indicated in green.

For fast scans in normal and parallel mode, this PSF structure is smeared by detector time constants and data averaging. Quantitative information on the PSF is given in Table 1.

Table 1: Results of fitting 2-dimensional gaussians to the PSF. Note these are fits to the full PSF including the lobes/wings. Position angles (east of North) are listed only for beams with clearly elongated core. The scan angle was 63° for these observations.

| Band | Speed arcsec/sec | FWHM arcsec | PA deg |
|---|---|---|---|
| Blue | 10 | 5.26×5.61 | |
| Blue | 20 | 5.46×5.76 | |
| Blue | 60 | 5.75×9.00 | 62.0 |
| Blue | 60/para | 5.86×12.16 | 63.0 |
| Green | 10 | 6.57×6.81 | |
| Green | 20 | 6.69×6.89 | |
| Green | 60 | 6.89×9.74 | 62.3 |
| Green | 60/para | 6.98×12.70 | 63.0 |
| Red | 10 | 10.46×12.06 | 7.6 |
| Red | 20 | 10.65×12.13 | 9.3 |
| Red | 60 | 11.31×13.32 | 40.9 |
| Red | 60/para | 11.64×15.65 | 53.4 |

These PSFs and derived quantities reflect the intrinsic optical quality of Herschel+PACS. In a scanmap reduction they will be very slightly smeared, in particular at short wavelengths, because of the data averaging on-board (from 40Hz to 10Hz sampling), but also due to detector time constants telescope pointing jitter and drifts.

For more detailed information on the PACS photometer PSF we refer to the PACS technical note **PICC-ME-TN-033**(version 0.3, Nov. 10, 2009)

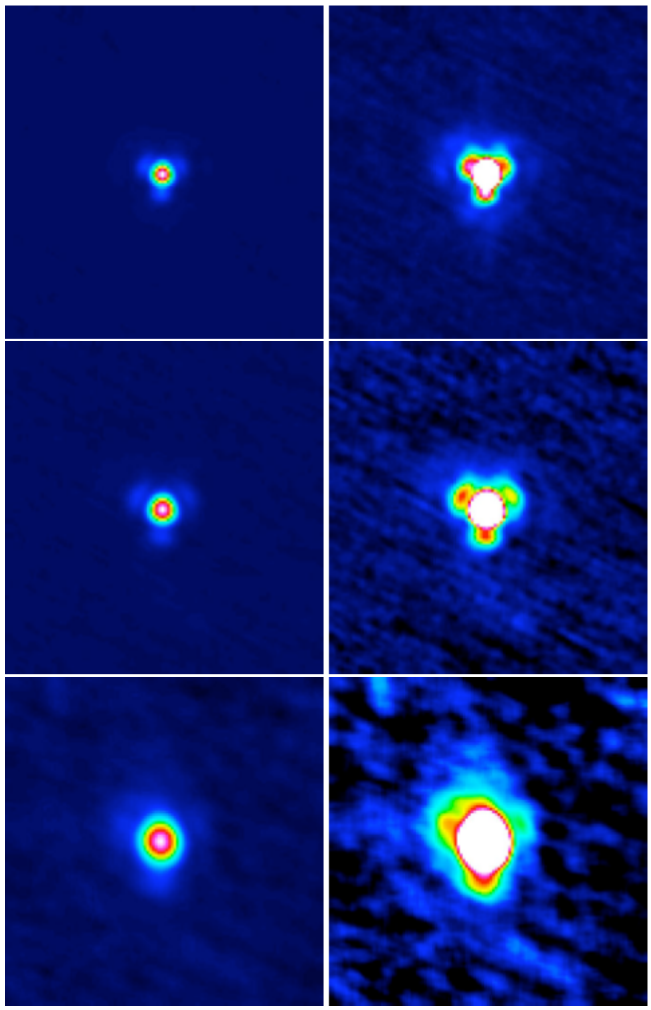

Figure 1: The photometer PSF in blue, green and red (top to bottom) derived from scans performed at 10 ″/s. Left-hand panels display the image with a linear scale up to the peak, while right-hand panels show up to 10% of the peak.

# 2 Flux calibration

The prime calibrators for PACS are a set of standard stars ($\alpha$ Boo, $\alpha$ Tau, $\alpha$ CMa, $\alpha$ Ceti & $\gamma$ Dra ...) These range from 0.6-15 Jy in the three filters. The secondary calibrators for PACS are additional, fainter standard stars and asteroids. The predicted fluxes for the standards are computed from model spectra (Decin & Eriksson, 2007 , A&A, 472, 1041) with color-terms added to mimic measured monochromatic fluxes of sources in the pass bands of PACS at the chosen reference wavelengths of the filters.

The calibration itself comprises: (i) flat-fielding, (ii) responsivity correction – conversion of engineering units, volts, to Jy/pixel, and (iii) gain drift correction to account to small drifts in gain with time.

For the 5 primary PACS calibrators, the measured absolute flux accuracy is within 5% of predicted values in the blue and green filters, and within 10% of the predicted values in the red filter. For the full set of primary and secondary standards, the measured absolute flux accuracy is within 10% in the blue and green, and better than 20% in the red filter.

The flux calibration of the PACS photometer assumes that :

1. The detectors are linear in the full dynamic flux range observable by PACS.
2. a spectral convention of $\nu \times f_\nu$ = constant and reference filter wavelengths at 70, 100 and 160 $\mu$m.
3. a set of celestial flux calibrators that are mostly stars and asteroids for which model spectra are available that allow either color-correction of the measured spectral densities in order to compare them with the predicted monochromatic model fluxes or computation of the expected measured spectral densities.

**NOTE: In the current public HIPE version 2.0 and also development versions 3.0 from the CIB (Continuous Integration Builds), which make use of the responsivity calibration file version 3 in the calibration tree, there is still an error in the flux scale which has to be corrected manually.**
The final reduced fluxes are too high and have to be scaled down by the following factors:

- **1.05 in the blue band,**
- **1.09 in the green band**
- **1.29 in the red band.**

This flux overestimation will be corrected in the next released valid calibration files as part of HIPE release 3.0.

The current version of the responsivity calibration can be checked by printing the relevant branch of calibration tree product in HIPE. E.g.

```
HIPE> calTree = getCalTree()
HIPE> print calTree.photometer
```

The version number appears in the 2nd column.

## 2.1 Aperture Corrections

The companion document, PICC-ME-TN-033 Version 0.3, details the aperture correction factors for the PACS photometry. The aperture correction are also listed in the table in section 7.

# 3 Sensitivity estimate

The preliminary estimates for observed sensitivities in the PACS bolometers suggests that it is within 10% of the values current values in HSpot (version 4.4 and earlier) for the blue and green filters. And, a factor up to 1.5x worse in the red filter. However, the achieved sensitivity is a strong function of data processing and scan strategy.

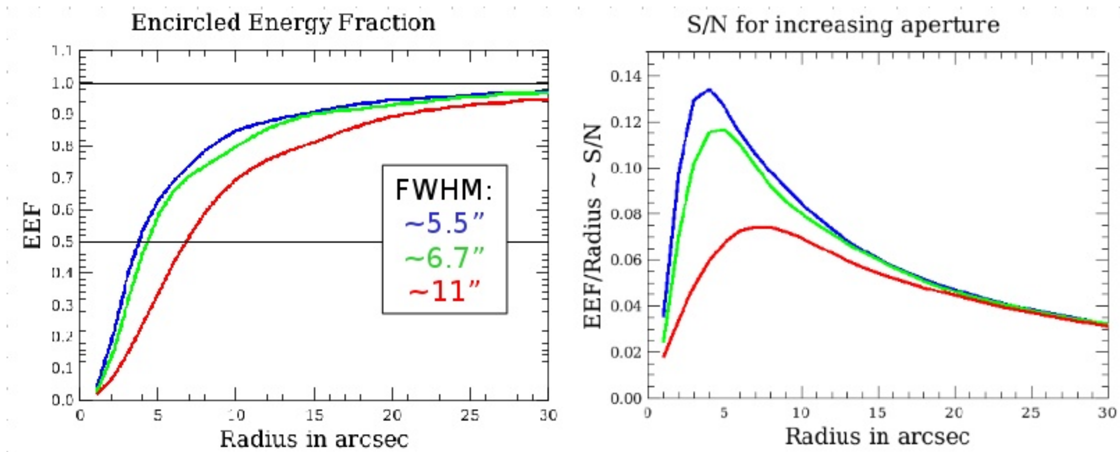


Figure 2: Left: Encircled energy fraction as a function of circular aperture radius for the three bands. Derived from slow scan OD160 Vesta data.The EEF fraction shown is normalized to the signal in aperture radius 60arcsec, with background subtraction done in an annulus between radius 61 and 70 arcsec. The right panel shows the corresponding S/N curve under the assumption that noise scales linearly with aperture radius. Note that this assumption is not met for scanmaps with 1/f noise.

The PACS blue and green filters are not confusion limited. The red filter is confusion bound at 5 mJy and below.

Based on inflight performance, we recommend that observers:

- Use the medium (20"/sec) scan speed over the slow (10"/sec) scan speed. The noise spectrum of PACS is such that the higher spatial mitigation from the faster scan speed trump any observing inefficiencies owing to turn-around times between scan legs. The fastest (60"/sec) scan speed should be used if a wide area is to be mapped.
- Use high-pass filter, where possible, for mitigating the so-called $1/\sqrt{f}$ noise and other detector drifts.
- Use concatenated cross-scans for observations that cannot benefit from high-pass filter reductions (e.g. fields with spatially complex, extended and diffuse emission).

# 4 Astrometric accuracy

The absolute pointing accuracy for Herschel is measured to be 2 arc-seconds at the 1-sigma level on pointed observations. However, deviations as large as 5 arc-seconds have been reported for some scan map observations.

Deviations of the actual telescope pointing from the scan legs (great circles in the sky) that is reported in the pointing product cause a smearing of the PACS PSF in the reconstructed scanmap, in particular in the blue/green bands. The jittering along scan legs is estimated to be usually around 1 arcsec level, therefore the effect is rather small even in the blue band.

## 4.1 Speed Bumps

The scan speed profile sometimes exhibits significant bumps above the average speed, see example in Figure 3 on two different scan legs. These events are relatively rare. The cause of these jumps has been traced down to warm star tracker (STR) CCD pixels. When a guide star of 5-6 magnitude approaches such a pixel, the STR gets confused, producing a wrong attitude estimate. During the speed bump the attitude is unreliable and could be up to several tens of arcsec off.

The time interval during the speed bumps shall currently not be used in the map projection. HSC is investigating methods to propagate the gyroscope angular rate to reconstruct the right attitude during these bump. In the near future the STR CCD shall be lowered to mitigate the effects of these warm pixels.

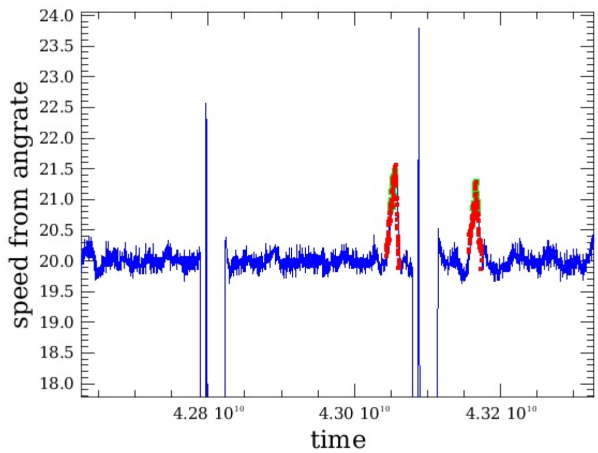


Figure 3: Example of two 'speed bumps' in a scan map, scanning at 20″/s.

## 5 Scan map pipeline processing issues

The current automatic pipeline processing provides reductions up to PACS level 1 and 2 products. At this point in the Herschel mission, the goal of the pipeline is to deliver useable, but not necessarily optimal, products. Instead, the automatic pipelines are optimized for stability, speed and delivering browse quality data. The pipelines are expected to mature as both the instrument effects and the understanding on how to mitigate said effects evolves.

The major data processing modules of the pipeline are discussed below:

- **Cosmic rays removal**: The default deglitching algorithm for PACS photometer is the multi-resolution median transform (MMT), which uses wavelet scales (Starck et al, 1998, PASP, 110, 193S) to differentiate between a cosmic ray hit and signal. The method produces reasonable results except for bright point-like sources (e.g. compact galactic nuclei, etc.) and fast (60"/sec) scan speeds. Under such conditions, MMT incorrectly masks point source cores. Users are advised to check the coverage map to look for any gaps in exposure depth at the location of point sources. The optional module, "2nd order deglitching" can be used in the interactive data processing as a replacement for MMT deglitching. "2nd order deglitching" uses spatial redundancy and sigma-clipping to reject cosmic ray hits.
- **Cross-talk correction**: The red bolometer array shows cross-talk between column 0 and 16. That is, when a source is present in column 16, its flux is also observed in column 0. Investigations on proper removal of cross-talks are underway. Users are currently advised to mask all signal in columns 0 and 16 to avoid any artifacts from cross-talk in the final maps when observing very bright (point-)sources
- **Responsivity / flat-field / gain drift corrections** : the responsivity version 3 has to be used with the correction factors given in section 2. The flat-field is still the one derived from ground based calibration campaigns and the gain drift correction is not implemented yet.
- **Offset drift correction** : Offset drift correction is performed by applying a simple high-pass filter on the data. This is adequate for point source fields, but not for structured field and may result in dark halo

artefacts. Increasing the filter window so that it covers a scan leg length already improves the map in the case of structured objects.

- **Map reconstruction**: Map reconstruction with `photProject` is a simple projection of the data cube on the map grid, considering the intersection areas of the native pixels with the map pixels. For this purpose the ra/dec coordinates of the four corners of each detector pixel in the cube are computed on the fly in `photProject`.

  An alternative, optimal map maker, MADmap (http://lanl.arxiv.org/abs/0906.1775), is provided in the data processing environment. This is a java implementation of the original MADmap C code. MADmap uses optimal map-making techniques to produce the best-fit solution for the final reconstructed maps. The primary advantage of MADmap is that it does not require the use of high-pass filter to mitigate 1/f noise and thus preserves spatial structures up to the size of final maps. Currently, MADmap is only available as an interactive tool and requires pre-processing to remove correlated signal drifts prior to optimal map reconstruction. MADmap additionally requires apriori knowledge of the detector noise properties (as the inverse of the time-time noise correlation matrix). Investigations on the noise filters are underway from the inflight data. Current version of the data processing environment relies of pre-launch estimates from ground-based tests. Users wishing to use MADmap for their data processing needs should contact the helpdesks at ESA or NHSC for further information.

# 6 Level 2 pipeline products for scan maps generated with HCSS 2.1

There are 3 types of products in the level 2 produced by the pipeline for the PACS photometer in scan map mode. MADmap as been disabled from the HSC pipeline with HCSS 2.0, hence the second product (HPPMMAP) is not available in recently processed scan maps observations.

These maps are produced by automatic pipeline scripts and shall only be considered as a **preview, and not for science directly**.

1. HPPPMAPB & HPPPMAPR stands for "Herschel Pacs Photometer PhotProject MAP Blue/Red"

   This refers to maps produced by the photProject task, i.e. a simple projection of each frames (10Hz), after running a temporal high-pass filter with a width of n=20 (i.e subtracting a median with a width of 2*n+1 frames.) This allows to filter a significant part of the 1/f noise at the expense of removing completely ALL spatial scales larger than this width (i.e. typically larger than 1 arcmin), and creating negative undershooting around bright sources along the scan direction.

   To preserve extended emission, the pipeline script shall be re-run with higher width in the high pass filtering and masking bright source when necessary or an alternative map-making algorithm/tool.

   This processing is mostly targeted to detect point-sources with good sensitivity.

   Scan maps are in Jy/pixel but the flux scale is off.

2. HPPMMAPB & HPPMMAPR stands for "Herschel Pacs Photometer Mad Map Blue/Red"

   The MADmap produced optimal map. This feature is currently disabled

3. HPPNMAPB & HPPNMAPR stands for for "Herschel Pacs Photometer Naive Map Blue/Red"

   Averaged signal map after pixel-to-pixel offset correction. This image is used by MADmap as its first value for the sky map and is subsequently improved and optimized iteratively as described above, hence the full optimized matrix inversion has not been performed on the data.

# 7 Tables of the encircled energy fractions

Table 2: Encircled energy fraction as a function of circular aperture radius for the three bands. Derived from slow scan OD160 Vesta data in the three photometer bands. The EEF fraction shown is normalized to the signal in aperture radius 60 arcsec, with background subtraction done in an annulus between radius 61 and 70 arcsec.

| | encircled energy fraction | | | Radius | encircled energy fraction | | |
|---|---|---|---|---|---|---|---|
| Radius [″] | blue | green | red | [″] | blue | green | red |
| 1 | 0.047 | 0.032 | 0.018 | 31 | 0.978 | 0.978 | 0.956 |
| 2 | 0.214 | 0.156 | 0.069 | 32 | 0.979 | 0.980 | 0.959 |
| 3 | 0.402 | 0.318 | 0.146 | 33 | 0.981 | 0.981 | 0.963 |
| 4 | 0.548 | 0.474 | 0.241 | 34 | 0.982 | 0.983 | 0.966 |
| 5 | 0.642 | 0.595 | 0.341 | 35 | 0.983 | 0.984 | 0.969 |
| 6 | 0.701 | 0.672 | 0.438 | 36 | 0.984 | 0.985 | 0.972 |
| 7 | 0.750 | 0.718 | 0.524 | 37 | 0.985 | 0.986 | 0.975 |
| 8 | 0.794 | 0.749 | 0.597 | 38 | 0.986 | 0.987 | 0.977 |
| 9 | 0.830 | 0.778 | 0.656 | 39 | 0.987 | 0.988 | 0.980 |
| 10 | 0.856 | 0.809 | 0.700 | 40 | 0.988 | 0.989 | 0.982 |
| 11 | 0.873 | 0.840 | 0.734 | 41 | 0.989 | 0.990 | 0.983 |
| 12 | 0.886 | 0.866 | 0.759 | 42 | 0.989 | 0.991 | 0.985 |
| 13 | 0.895 | 0.885 | 0.781 | 43 | 0.990 | 0.992 | 0.987 |
| 14 | 0.904 | 0.900 | 0.801 | 44 | 0.991 | 0.993 | 0.988 |
| 15 | 0.913 | 0.910 | 0.820 | 45 | 0.992 | 0.994 | 0.990 |
| 16 | 0.922 | 0.917 | 0.838 | 46 | 0.992 | 0.994 | 0.991 |
| 17 | 0.931 | 0.923 | 0.855 | 47 | 0.993 | 0.995 | 0.992 |
| 18 | 0.938 | 0.928 | 0.871 | 48 | 0.993 | 0.996 | 0.993 |
| 19 | 0.945 | 0.932 | 0.885 | 49 | 0.994 | 0.996 | 0.994 |
| 20 | 0.949 | 0.938 | 0.897 | 50 | 0.995 | 0.997 | 0.995 |
| 21 | 0.953 | 0.943 | 0.907 | 51 | 0.995 | 0.997 | 0.996 |
| 22 | 0.957 | 0.948 | 0.916 | 52 | 0.996 | 0.997 | 0.997 |
| 23 | 0.960 | 0.954 | 0.923 | 53 | 0.997 | 0.998 | 0.998 |
| 24 | 0.963 | 0.958 | 0.929 | 54 | 0.997 | 0.998 | 0.998 |
| 25 | 0.966 | 0.963 | 0.934 | 55 | 0.998 | 0.998 | 0.999 |
| 26 | 0.968 | 0.966 | 0.938 | 56 | 0.998 | 0.999 | 0.999 |
| 27 | 0.970 | 0.970 | 0.942 | 57 | 0.999 | 0.999 | 0.999 |
| 28 | 0.973 | 0.972 | 0.946 | 58 | 0.999 | 0.999 | 0.999 |
| 29 | 0.974 | 0.975 | 0.949 | 59 | 1.000 | 1.000 | 1.000 |
| 30 | 0.976 | 0.977 | 0.953 | 60 | 1.000 | 1.000 | 1.000 |